

Synovial Fibroblasts of Patients with Rheumatoid Arthritis Attach to and Invade Normal Human Cartilage when Engrafted into SCID Mice

Ulf Müller-Ladner,* Jörg Kriegsmann,*
Barry N. Franklin,* Shigeru Matsumoto,*
Thomas Geiler,* Renate E. Gay,*† and
Steffen Gay*†

From the Division of Clinical Immunology and Rheumatology, *Department of Medicine, The University of Alabama at Birmingham, Birmingham, Alabama, and the Center for Experimental Rheumatology,† University Hospital Zurich, Switzerland

Rheumatoid arthritis (RA) has been thought to be largely a T-cell-mediated disease. To evaluate the role of T-cell-independent pathways in RA, we examined the interaction between isolated RA synovial fibroblasts and normal human cartilage engrafted into SCID mice in the absence of T cells and other human cells. The expression of cartilage-degrading enzymes and adhesion molecules was examined by immunohistochemistry and in situ hybridization techniques. The RA synovial fibroblasts invaded the cartilage and kept their transformed-appearing cellular shape. They expressed VCAM-1 and produced the cathepsins L and B at the site of invasion. We conclude that RA synovial fibroblasts maintain their invasive and destructive behavior over longer periods of time in the absence of human T cells, indicating that T-cell-independent pathways play a significant role in rheumatoid joint destruction. (Am J Pathol 1996, 149:1607–1615)

Rheumatoid arthritis (RA) is characterized by a progressive destruction of the affected joints. Although RA is a rather common disease, its pathophysiology is poorly understood. Well known hallmarks of RA are synovial hyperplasia, inflammation, and autoimmune phenomena.¹ Among the theories addressing the question of which cellular actions and interactions cause RA, T-cell-dependent pathways were believed to play the most crucial role. However, experimental approaches in the past several years sup-

port the novel concept that T-cell-independent pathways may contribute significantly to RA.^{1,2}

Microscopic examination generally shows a considerable increase in cell number and thickness of synovial tissue and an invasive growth of the diseased synovium into the adjacent cartilage and bone. Type A (macrophage-like) and especially type B (fibroblast-like) synoviocytes are the cell types of the lining layers of the synovium that actually invade and destroy cartilage and bone by the production of matrix-degrading enzymes such as collagenase, stromelysin, and cathepsins.^{3–11} The attachment and adherence of the synovial fibroblasts to cartilage and bone is most likely facilitated by the expression of adhesion molecules. Among these, vascular cell adhesion molecule (VCAM)-1, a member of the immunoglobulin family, is expressed by synovial fibroblasts in the lining layer of RA synovium.^{12–14} The microscopic appearance of the synovial fibroblasts invading the cartilage and bone is different from those in normal synovium. Their histological and ultrastructural morphology is frequently that of transformed cells.¹⁵ Recent results on the molecular level suggest that this alteration in the cell structure and metabolism could be caused by the activation of (proto-) oncogenes such as *c-myc*, *fos*, and *ras* (for Review see Ref. 16).

Based on the observation that synovial cells are able to form pannus-like structures when implanted in nude mice¹⁷ and that various *in vitro* models showed the potential of synovial fibroblasts to attach and subsequently invade human cartilage,^{18,19} we have demonstrated the value of a SCID mouse

Supported by a grant from Sankyo Inc. U. Müller-Ladner and J. Kriegsmann were supported by a grant of the German Academic Exchange Service and contributed equally to this article.

Accepted for publication July 1, 1996.

Present address of U. Müller-Ladner: Department of Internal Medicine I, University of Regensburg, 93042 Regensburg, Germany.

Address reprint requests to Dr. Steffen Gay, Center for Experimental Rheumatology, University Hospital, Gloriastrasse 25, CH-8091 Zurich, Switzerland.

model for examining the interaction between human synovium and cartilage in the absence of circulating human blood components.²⁰ In contrast to synovium of patients with osteoarthritis (OA), synovium derived from patients with RA deeply invaded cartilage and expressed mRNA for matrix-degrading enzymes at the site of destruction.²⁰ Based on these results, we used the SCID mouse model to determine whether isolated synovial fibroblasts of patients with RA (multiple-passaged, prolyl 4-hydroxylase²¹-positive, CD68-negative) are capable of degradative invasion into normal human cartilage devoid of normal matrix components and other synovial cells. To answer this question, we established a new implantation technique that kept the synovial fibroblasts in close contact with the cartilage in the initial phase of co-implantation in the SCID mouse.

To further characterize the properties of fibroblasts derived from patients with RA and determine the pathophysiological impact of these cells on this disease, our experiments were designed to address the following questions. First, we sought to demonstrate the isolated RA fibroblasts' invasive growth into normal human cartilage and ask whether this growth was more aggressive compared with that of OA fibroblasts, skin fibroblasts, or normal fibroblasts. Second, do the RA fibroblasts keep their transformed appearance in this environment? And finally, do RA fibroblasts remain activated over an extended period of implantation time, as assessed by the expression of the adhesion molecule VCAM-1 and the production of matrix-degrading cathepsins.

Materials and Methods

Preparation of Fibroblasts and Cartilage

Synovial fibroblasts were obtained from biopsy of synovial tissue from four patients with RA, of whom all met the revised RA criteria of the American College of Rheumatology, during an active stage of the disease. After enzymatic digestion using Dispase (Boehringer Mannheim, Indianapolis, IN) in a 1.5% solution in Joklicks medium, the fibroblasts were grown in culture flasks in Dulbecco's modified Eagle's medium/Cellgro (Mediatech, Washington, DC) containing 10% fetal calf serum (Gibco Life Technologies, Grand Island, NY). Cells were harvested after three to six passages and tested for mycoplasma before implantation. Immediately before implantation, the fibroblasts were trypsinized (Mediatech) in 0.05% trypsin, containing 0.5 mmol/L EDTA, spun down, and resuspended in 1 ml of phosphate-buffered saline (Mediatech). Synovial OA fibroblasts

from patients who were undergoing joint surgery, skin fibroblasts from foreskins of newborns, and normal synovial fibroblasts from patients undergoing non-arthritic leg amputations were prepared in the same way. Human normal cartilage was obtained from patients undergoing either cardiac surgery (rib cartilage) or non-arthritic amputations (knee cartilage).

SCID Mice

SCID mice were obtained from a germ-free breeding colony at The University of Alabama at Birmingham (Dr. J. Kearney, Department of Microbiology) and examined for macroscopic anomalies before and during surgery as well as for macro- and histopathological abnormalities after sacrifice.

Implantation

Implantation of both fibroblasts and cartilage under the renal capsule of the SCID mice was performed under sterile conditions as previously described.²⁰ In addition, we used a newly developed sponge technique in which fibroblasts and cartilage were first inserted microscopically into a cavity of inert sterile gel sponge (Upjohn, Kalamazoo, MI) in a total volume of 2 mm³ to keep cells and cartilage in close contact and then co-implanted in a pocket of the surgically opened renal capsule. A total of 16 SCID mice were used for the implantations. Normal human cartilage and RA synovial fibroblasts were implanted in 6 mice. Control groups consisted of co-implants performed with OA fibroblasts (5 mice), skin fibroblasts (3 mice), and normal fibroblasts (2 mice). Dissection of the mice took place after 60 days (preliminary data showed an initial invasive growth after 30 days when RA fibroblasts were used).

Histological Evaluation and Immunohistochemistry

Immediately after explantation, the implants together with a section of the adjacent kidney were snap-frozen in OCT Tissue Tek (Miles Laboratories, Elkhart, IN) in liquid nitrogen and stored at -70°C. The implants were examined by techniques established in our laboratory.^{11,14,20,22} Using standard hematoxylin and eosin (H&E) staining, each specimen was evaluated for the degree of destruction of the implanted cartilage. Scores with grades 0 to 4 were used, ranging from no visible destruction (grade 0) to 40% destruction (grade 4). Statistical analysis was

performed using the Mann-Whitney *U* test for non-parametric data, and *P* values <0.01 were regarded as significant. Different immunohistochemistry techniques according to the nature of the antigen and the applicability of the specific antibody were performed for the detection of cathepsins B, D, and G as well as for VCAM-1, the fibroblast enzyme prolyl 4-hydroxylase,²¹ the macrophage antigen CD68,¹⁴ and human basement collagen type IV.²³ Nonradioactive *in situ* hybridization was performed for cathepsin L and VCAM-1.

Diaminobenzidine (DAB)/Peroxidase Technique

The DAB/oxidase technique was used for immunohistochemical analysis of cathepsin B and D. Sections were cut (4–6 μ m), fixed for 5 minutes in pure acetone, and air dried. To inhibit endogenous peroxidase, the sections were washed in 1% H₂O₂ for 5 minutes. After a blocking step with 4% milk and 2% normal horse serum in Tris buffer (Tris/NaCl, pH 7.5) for 30 minutes, the sections were washed in Tris buffer and the primary antibodies, mouse monoclonal anti-human cathepsin B (Oncogene, Cambridge, MA) or anti-cathepsin D (Dako Corp., Carpinteria, CA) were applied to the sections in 2% milk Tris buffer for 1 hour at room temperature, diluted according to the manufacturer's recommendations. After washing three times in Tris buffer, the sections were incubated with the appropriate secondary peroxidase-labeled antibodies (Jackson ImmunoResearch Laboratories, West Grove, PA) for 30 minutes at room temperature. After a washing step in Tris buffer, DAB (Dako) was applied at a concentration of 1 mg/ml in cacodylate buffer, pH 7.5, for 30 minutes at room temperature. Then the sections were incubated with DAB in a 0.01% H₂O₂ solution for 1 hour at room temperature, washed in Tris buffer, and mounted with gel mount (Biomedex, Foster City, CA).

Alkaline Phosphatase Anti-Alkaline Phosphatase (APAAP) Method

Immunohistochemistry was also performed using the APAAP method with mouse monoclonal antibodies against human basement membrane collagen type IV,²³ the fibroblast enzyme prolyl 4-hydroxylase²¹ (Dako), and human macrophages (anti-CD68, Dako). Sections or cells were fixed for 5 minutes in acetone, covered with a 4% milk, 2% normal horse serum Tris buffer for 30 minutes at room temperature to block nonspecific binding, washed in Tris buffer, and incubated for 45 minutes at room temperature with the

primary antibodies diluted 1:50 to 1:100 in Tris buffer. The slides were rinsed in Tris buffer and incubated for 30 minutes at room temperature with a secondary goat anti-mouse IgG antibody (Jackson) in a 1:400 dilution in Tris buffer. Incubation with the APAAP complex (Dako) for 30 minutes at room temperature (dilution 1:100 in Tris buffer) was followed by the addition of substrate using the new fuchsin method (Dako). The color development was stopped, after examining the slides microscopically, by adding a mixture of 10 mmol/L Tris buffer and 1 mmol/L EDTA. The slides were mounted immediately.

Immunogold/Silver Technique

This method was used for the detection of VCAM-1 antigen. Snap-frozen sections were cut (4 to 6 μ m), fixed for 5 minutes in acetone, and covered with a 4% milk, 2% normal horse serum Tris buffer for 30 minutes at room temperature to block nonspecific binding. Then, slides were washed in Tris buffer and incubated for 45 minutes at room temperature with anti-human VCAM-1 antibody (R&D Systems, Minneapolis, MN) in Tris buffer, diluted according to the manufacturer. The slides were rinsed in Tris buffer and incubated for 30 minutes at room temperature with a biotinylated goat anti-mouse antibody (Jackson) diluted 1:600 in Tris buffer. After a washing step in Tris buffer, sections were incubated for 45 minutes with peroxidase-conjugated streptavidin (Jackson) diluted 1:600 in Tris buffer. After a rinsing step, 6-nm-gold-labeled goat anti-horseradish peroxidase (Jackson) diluted 1:40 in Tris buffer was applied. For photochemical silver amplification, the sections were incubated in a 1:1 mixture of double-distilled deionized water (Fisher Scientific, Pittsburgh, PA) and 0.05 mol/L citrate buffer (pH 3.8) containing 250 mg hydroquinone (Fluka, Buchs, Switzerland) for 5 minutes at room temperature. The sections were immediately transferred into 100 ml of a 50% hydroquinone (in citric acid, see above) and 50% silver acetate (Fluka, 100 mg dissolved in 50 ml of double-distilled water) solution. After 18 minutes, the sections were quickly rinsed with distilled water and placed in photographic fixative (Kodak, Rochester, NY) for 2 minutes, rinsed thoroughly with distilled water, and mounted with gel mount.

In Situ Hybridization

Preparation of Riboprobes

The cathepsin L riboprobes were prepared by standard procedures.⁸ Briefly, cDNA fragments

were cloned into the Bluescript SK+ vector (Stratagene, La Jolla, CA). After a miniprep insert check, a large-scale preparation of the cathepsin L insert-containing plasmids was performed after transformation of NM 522 *Escherichia coli* bacteria using the calcium chloride procedure. The plasmids were extracted and purified using Nucleobond-AX columns (Macherey-Nagel, Düren, Germany) and linearized to permit generation of antisense and sense riboprobes.

Antisense and sense RNA probes were transcribed by T3 and T7 RNA polymerase using a commercially available RNA transcription kit according to the manufacturer's protocol (Stratagene). Probes were labeled with digoxigenin-UTP (Boehringer Mannheim). The proportion of labeled to unlabeled UTP in the reaction buffer was 1:2. The efficiency of the transcription was checked by transfer of the probe to a nitrocellulose membrane (Gibco) after electrophoresis and detection of the labeled RNA using the nucleic acid detection kit (Boehringer Mannheim) according to the manufacturer's protocol.

In Situ Hybridization

All of the described steps were performed in an RNase-free environment. Frozen sections (4 to 6 μm) were cut and fixed in 3% buffered paraformaldehyde for 1 hour at room temperature. The sections were rinsed in 2X standard saline citrate (SSC; 0.3 mol/L NaCl, 0.03 mol/L sodium citrate) followed by incubation in 2X SSC, 0.1 mol/L triethanolamine/HCl, pH 8.0 (Sigma Chemical Co., St. Louis, MO), 0.25% acetic anhydride (Fisher Scientific, Springfield, NJ) for 15 minutes at room temperature. After a rinsing step with 0.1 mol/L triethanolamine/HCl (pH 8.0), the prehybridization was performed in a prehybridization buffer containing 2.5 ml of formamide (Sigma), 1 ml of 20X SSC, 0.1 ml of 50X Denhardt's solution (Sigma), 0.25 ml of herring sperm DNA (Sigma; 10 mg/ml stock solution, heat denatured for 10 minutes), 0.125 ml of yeast tRNA (Boehringer Mannheim; 10 mg/ml stock solution), and 1.0 ml of 50% dextran sulfate (Sigma). After the prehybridization, a previously tested amount of digoxigenin-labeled antisense or sense probe (for control) was applied to the tissue specimens in 15 μl of prehybridization buffer. The slides were sealed with nail polish and hybridized for 3 hours in a humid chamber at 50°C. After transferring the slides out of the RNase-free chambers, they were washed at room temperature, twice with 2X SSC and once with STE buffer (500 mmol/L NaCl, 1 mmol/L EDTA, 20 mmol/L Tris/HCl, pH 7.5). After

digestion for 1 hour at 37°C with 20 g/ml RNase A (Boehringer Mannheim) in STE, slides were rinsed with 2X SSC, 50% formamide for 5 minutes, followed by 1X SSC, 0.1% sodium dodecyl sulfate (SDS) for 10 minutes and 0.5X SSC, 0.1% SDS for 15 minutes. All rinses were performed in a water bath at 50°C.

Immunological Detection

The slides were washed in Tris buffer and incubated in Tris buffer containing 2% normal horse serum to block nonspecific binding for 30 minutes at room temperature followed by incubation with anti-digoxigenin-AP-antibody complex (5-nm colloidal gold, EM sheep; Goldmark Biologicals, Phillipsburg, NJ) in Tris buffer containing 1% normal horse serum. Signal detection by the immunogold/silver technique was performed as described above.

Controls

Before implantation, the cells were tested for contamination with type A (macrophage-like) synoviocytes using anti-fibroblast antibodies (Dako²¹) as positive control and anti-CD68 (Dako) antibodies as negative control in the APAAP immunocytochemistry assay. None of the implanted fibroblasts expressed the CD68 marker, and >95% stained positively for the fibroblast enzyme prolyl 4-hydroxylase (data not shown) and were considered homogeneous type B synoviocytes, as previously described.²⁴ Anti-cathepsin G antibodies (Dako) were used to exclude contamination of the type B synoviocytes with neutrophils. Negative controls were performed in each of the techniques described above by omitting the primary antibody or by using the sense probe in the *in situ* hybridization assay.

Results

Except for one mouse in the RA group, which died due to a neoplastic process in the pancreas, all mice survived surgery and demonstrated no problems with wound healing. After 60 days, all implanted pieces of cartilage could be retrieved and were still located under the renal capsule. Only minimal scarring and no necrosis was observed around the implants. Before specific immunohistochemistry and *in situ* hybridization, immunohistochemistry excluded the presence of human macrophages, human capillaries, or neutrophils (data not shown).

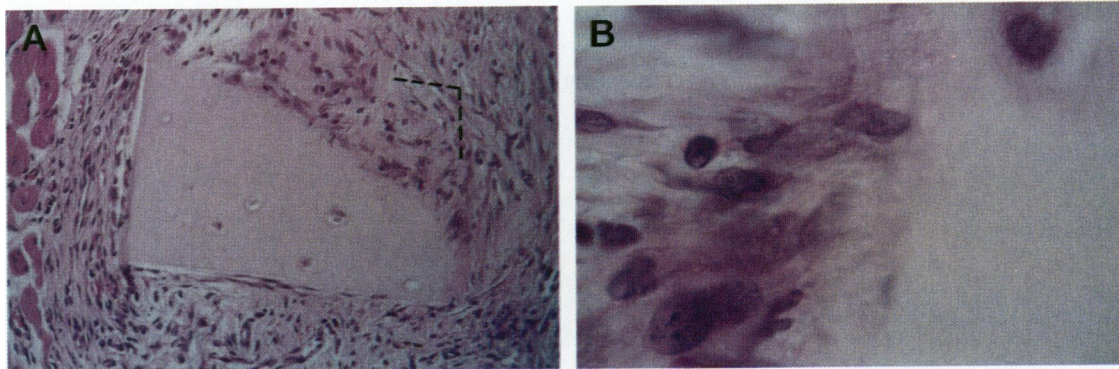


Figure 1. A: RA fibroblasts engrafted together with normal human cartilage under the renal capsule of a SCID mouse. Note the destruction of the cartilage (--- delineates original shape) by the RA fibroblasts after 60 days of implantation and the diffuse margin at the two sides of invasion. H&E; original magnification, $\times 125$. **B:** Detail of a serial section of the same tissue as shown in A. Note the transformed-appearing phenotype of the spindle-shaped RA fibroblasts. They are characterized by a large nucleus containing prominent nucleoli and an abundant cytoplasm. H&E; original magnification, $\times 1260$.

Histology

Microscopically, all implants performed with RA fibroblasts (5 of 5) showed an intensive, directed invasive growth into the cartilage (Figure 1A). The invading, predominantly spindle-shaped fibroblasts were transformed in appearance with large pale nuclei containing prominent nucleoli and expressing an abundant cytoplasm (Figure 1B). At the sites of invasion, the margins between the fibroblasts and the cartilage were diffuse, suggesting a process of marked degradation of the cartilage components by enzymes released from the fibroblasts. In contrast, the implants performed with OA fibroblasts showed only isolated, small regions of superficial erosion of the cartilage (Figure 2A), and none of the implants performed with foreskin and normal fibroblasts revealed any sign of invasion (Figure 2B). These results are summarized in Table 1. In all 15 implants, the response of the surrounding mouse connective tissue toward the implants was limited with limited

murine vascular proliferation observed. Interestingly, large remnants of the sponge were found only in some of the non-RA specimens that lacked any sign of proliferation of the implanted fibroblasts (Figure 2B).

Production of Matrix-Degrading Enzymes

All specimens showing invasion of fibroblasts into the adjacent cartilage were then examined for the presence of cathepsins and compared with the control implants. Matrix-degrading enzymes (cathepsins B, D, and L) were detected in all RA implants at the site or close to the areas of invasion. In general, the location and the distribution of the different cathepsins differed within the same specimen but showed a similar pattern in all examined RA implants. Cathepsin L mRNA was found in RA fibroblasts adjacent to the cartilage at sites of pocket-shaped zones of invasion, forming small clusters (Figure 3). In contrast, the number and distribution of fibroblasts expressing

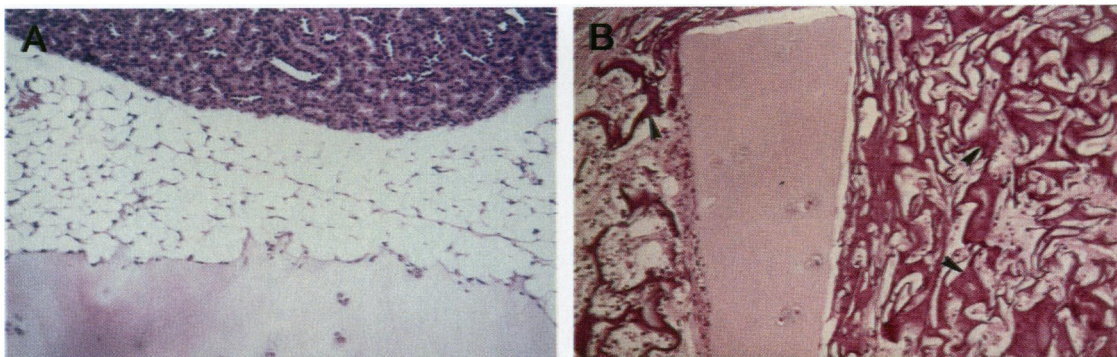


Figure 2. A: OA fibroblasts engrafted together with normal human cartilage under the renal capsule of a SCID mouse. Only isolated, shallow erosions can be observed at the surface of the cartilage. This figure also illustrates the implantation site under the renal capsule. H&E; original magnification, $\times 125$. **B:** Skin fibroblasts engrafted together with normal human cartilage under the renal capsule of a SCID mouse. Note the complete lack of invasive growth compared with Figure 1. In addition, this figure demonstrates the implantation technique with the fibroblasts and the cartilage located in a pocket of the inert dental sponge (arrowhead). H&E; original magnification, $\times 125$.

Table 1. Degree of Invasion into Normal Human Cartilage by Different Types of Human Fibroblasts Engrafted under the Renal Capsule of SCID Mice

Fibroblast origin	Grade of destruction of the adjacent cartilage in each of the single implants (1 to 5)					Mean \pm SEM
	1	2	3	4	5	
RA synovium	3.5	1	3	2.5	2	2.4 \pm 0.96*
OA synovium	0	0.25	0	0.25	0	0.1 \pm 0.14
Normal skin	0	0	0			0 \pm 0
Normal synovium	0	0				0 \pm 0

Scoring: 0, not visible; 1, <10%; 2, 11 to 20%; 3, 21 to 30%; 4, 31 to 40% destruction of the cartilage.
 * $P < 0.01$ as compared with OA fibroblasts.

cathepsin B protein was different. Cathepsin B was produced by numerous RA fibroblasts close to and directly attached to the cartilage. Frequently, single cathepsin-B-positive cells spearheading into the cartilage were observed (Figure 4A). In contrast, the number of RA fibroblasts expressing cathepsin D was distinctly lower, and most of the cells were not in

close contact with the cartilage (Figure 4A). None of the control specimens showed a measurable amount of cathepsin production or invasive growth based on the limited erosion of the cartilage surface. Representative examples of results using OA and skin fibroblasts are shown in Figure 5, A and B, demonstrating the lack of signal for cathepsin B.

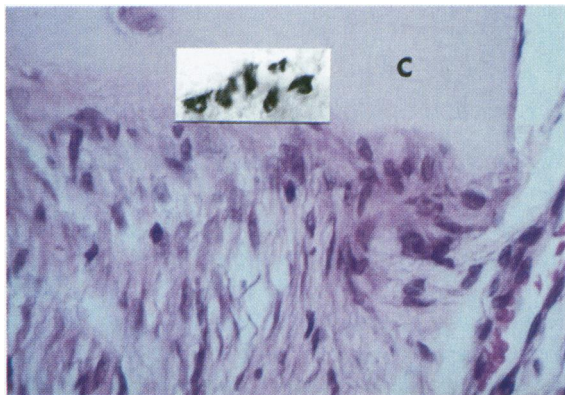


Figure 3. Detail of a serial section of the same tissue section as in Figure 1A. H&E; original magnification, $\times 800$. Inset: Cluster of RA synovial fibroblasts strongly expressing cathepsin L mRNA at the site of invasion into the adjacent cartilage (C). Immunogold/silver development of the gold-labeled anti-digoxigenin antibodies detecting the digoxigenin-UTP molecules within the hybridized cathepsin L probes. Original magnification, $\times 800$.

Expression of VCAM-1 in RA Implants

Strong expression of VCAM-1 protein, which is normally present in the lining layer of RA synovial tissue in abundant amounts, could be detected only in single RA fibroblasts at the site of invasion (Figure 6). Interestingly, none of the *in situ* techniques used for the detection of VCAM-1 mRNA revealed a specific signal, presumably due to a low copy number of mRNA.

Discussion

The goal of this study was to evaluate the properties of isolated synovial fibroblasts from patients with RA with regard to their destructive capabilities toward normal human cartilage *in vivo*. Our technical ap-

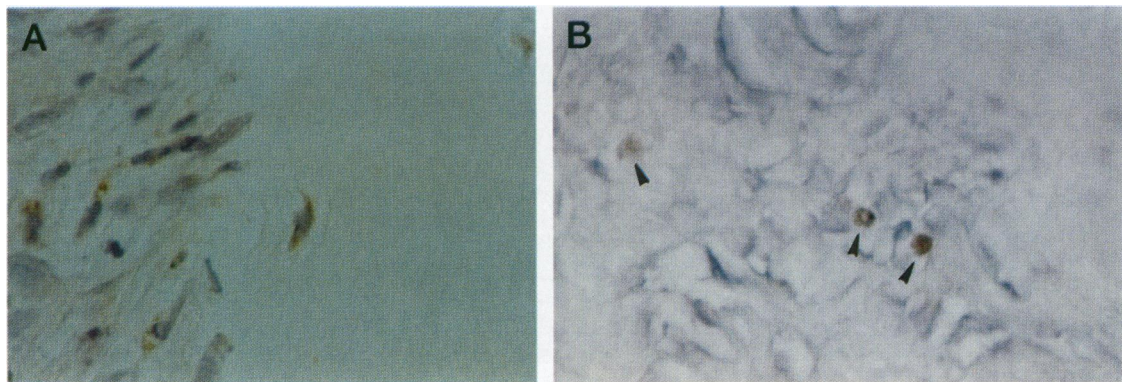


Figure 4. A: Expression of cathepsin B by numerous RA synovial fibroblasts. Note the spearheaded zone of invasion with the mostly deeply invasive cells strongly expressing cathepsin B. brown staining, DAB immunohistochemistry, counterstaining with hematoxylin; original magnification, $\times 640$. B: Single RA synovial fibroblasts producing cathepsin D (arrowheads) as demonstrated by DAB immunohistochemistry. Note that the cells directly at the site of invasion do not express cathepsin D.

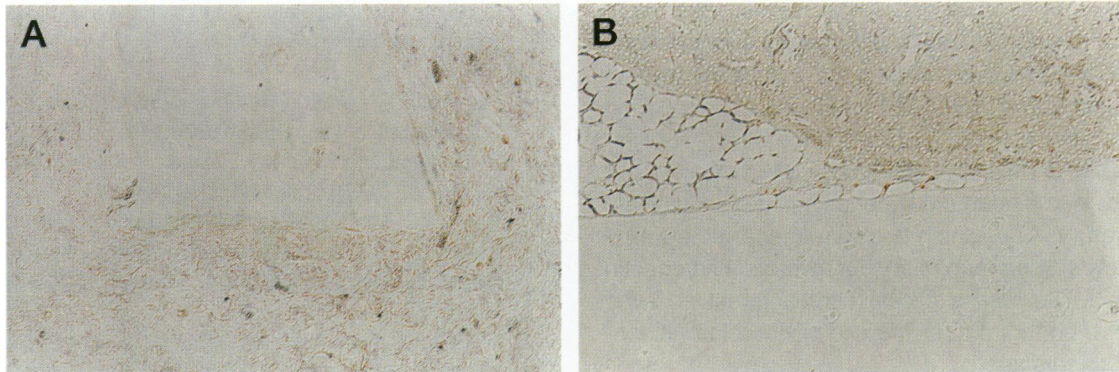


Figure 5. Absence of cathepsin B production in OA and foreskin fibroblasts. A: Results of an implant performed with OA fibroblasts. B: Results for the same procedure when foreskin fibroblasts were used. Immunogold/silver immunohistochemistry; original magnification, $\times 125$.

proach was based on the results of previous experiments that demonstrated that the SCID mouse model, lacking allogenic immune responses, provides an ideal environment to study the interaction of human tissue components. Rendt et al²⁵ demonstrated that implanted synovium maintains its histological and phenotypic properties when implanted under the renal capsule. In addition, RA synovium not only survives more than 200 days when engrafted into SCID mice, it also invades and destroys co-implanted normal human cartilage in the absence of cells of the human immune system.²⁰

The advantages of the co-implantation technique allows us more directly to address questions regarding the role of the synovial fibroblast in the pathogenesis of RA.

First, RA synovial fibroblasts retain their transformed appearance on limited passage in cell culture and when engrafted in SCID mice. OA fibroblasts, foreskin fibroblasts, and normal fibroblasts did not display this peculiar shape under the described experimental conditions. Although the term transformation is specific for malignant cells, in this

regard it does not relate to uncontrolled proliferation but rather describes a state of cellular activation combined with a transformed-appearing cellular phenotype. Interestingly, other reports indicate that RA synovial fibroblasts do not have an increased rate of proliferation *in vitro*²⁶ or *in vivo*.²⁷ Oncogene- or virus-derived gene sequences incorporated into the synovial cell DNA, as shown in an experimental model,²⁸ may play a role in inducing such an appearance.¹⁶

Second, even after several passages in cell culture and 60 additional days in the SCID mouse, RA synovial fibroblasts are readily capable of producing matrix-degrading enzymes. This might be the most significant result of this study, as the release of joint-destructive proteases such as cathepsins ultimately determines the clinical outcome of the disease. In the case of RA, it has been shown that the cysteine proteinases, cathepsin L, a major *ras*-induced protein,⁸ and cathepsin B⁹ are strongly expressed in RA synovial cells at the site of invasion. Expression of these two cathepsins appears to be essential features of invading synovial fibroblasts as demonstrated in our experiments and when compared with the differential expression of cathepsin D. The role of cathepsin D still remains to be elucidated,¹¹ although it has been suggested that cathepsin D may serve as an enzymatic activator of the zymogen forms of cathepsins L and B.²⁸

Interestingly, the predominance of cathepsin L, and not cathepsin D, at the site of invasion was similar to the results of Geiler et al²⁰ when complete synovium was engrafted. This finding indicates that the synovial matrix has little influence on the production of certain cathepsins by RA synovial fibroblasts. Our results also indirectly illustrate the importance of matrix metalloproteinases for the degradation of cartilage, as none of the control fibroblasts expressed detectable amounts of these enzymes.

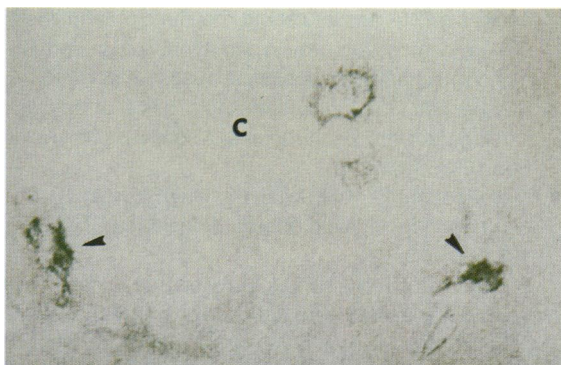


Figure 6. Demonstration of VCAM-1 protein in RA synovial fibroblasts at the site of invasion into cartilage. Two spindle-shaped fibroblasts strongly express VCAM-1 (arrowheads). C, cartilage. Immunogold/silver immunohistochemistry; original magnification, $\times 800$.

Third, RA synovial fibroblasts maintain their capability to express VCAM-1, one of the adhesion molecules most intensively expressed in the lining layer of RA synovium.^{13,14} VCAM-1 was originally described in endothelial cells,²⁹ facilitating the homing of lymphocytes to sites of inflammation in RA synovium.³⁰ It is known to bind to the lymphocyte integrin very late antigen (VLA)-4, which is also a ligand for an alternatively spliced form of the matrix protein fibronectin CS-1.³¹ The results shown here suggest an even more important role at the site of fibroblast attachment to cartilage.

Taken together, these data demonstrate that at least three matrix-degrading enzymes (cathepsins B, D, and L) were produced and were present at the site of RA synovial fibroblast invasion into human cartilage after 60 days of growth. VCAM-1 protein was located at the same sites in cells attached to the cartilage, suggesting a role in facilitating cell adhesion. In addition, the use of an inert gel sponge demonstrated a most useful method to replace the synovial matrix as a carrier for synovial fibroblasts providing an environment devoid of stimulatory or inhibitory effects of other cellular and matrix components.

Our data demonstrate for the first time that isolated synovial fibroblasts derived from patients with RA, but not fibroblasts from patients with OA, foreskin fibroblasts, or normal fibroblasts, maintain their invasive and destructive capabilities toward normal human cartilage after several passages in cell culture or when engrafted under the renal capsule of SCID mice.

The results support the hypothesis that T-cell-independent pathways play a significant role in the pathogenesis of RA³² and that the synovial fibroblast is the major synovial cell responsible for the continuous destruction of cartilage and bone.

References

1. Gay S, Gay RE, Koopman WJ: Molecular and cellular mechanisms of joint destruction in rheumatoid arthritis: two cellular mechanisms explain joint destruction? *Ann Rheum Dis* 1993, 52:S39-S47
2. Zvaifler NJ, Firestein GS: Pannus and pannocytes: alternative models of joint destruction. *Arthritis Rheum* 1994, 37:783-789
3. Woolley DE, Crossley MJ, Evanson JM: Collagenase at sites of cartilage erosion in the rheumatoid joint. *Arthritis Rheum* 1977, 20:1231-1239
4. McCachren SS, Haynes BF, Nield JE: Localization of collagenase mRNA in rheumatoid arthritis synovium by *in situ* hybridization histochemistry. *J Clin Immunol* 1990, 10:19-27
5. Krane SM, Conca W, Stephenson ML, Amento EP, Goldring MB: Mechanisms of matrix degradation in rheumatoid arthritis. *Ann NY Acad Sci USA* 1990, 580:350-354
6. Maciewicz RA, Wotton SF, Etherington DJ, Duance VJ: Susceptibility of the cartilage collagens type II, IX, and XI to degradation by the cysteine proteinases, cathepsin B and L. *FEBS Lett* 1990, 269:189-193
7. Nguyen Q, Mort JS, Roughley PJ: Cartilage proteoglycan aggregate is degraded more extensively by cathepsin L than by cathepsin B. *Biochem J* 1990, 266:569-573
8. Trabant A, Aicher WK, Gay RE, Sukhatme VP, Nilson-Hamilton M, Hamilton RT, McGhee JR, Fassbender HG, Gay S: Expression of the collagenolytic and *ras*-induced cysteine protease cathepsin L and proliferation-associated oncogenes in synovial cells of MRL/l mice and patients with rheumatoid arthritis. *Matrix* 1990, 10:349-361
9. Trabant A, Gay RE, Fassbender HG, Gay S: Cathepsin B in synovial cells at the site of joint destruction in rheumatoid arthritis. *Arthritis Rheum* 1991, 34:1444-1451
10. Firestein GS, Paine M: Expression of stromelysin and TIMP in rheumatoid arthritis synovium. *Am J Pathol* 1992, 140:1309-1314
11. Keyszer GM, Heer AH, Kriegsmann J, Geiler T, Trabant A, Keysser M, Gay RE, Gay S: Comparative investigation of cathepsin L, cathepsin D, and collagenase mRNA expression in synovial tissue of patients with rheumatoid arthritis and osteoarthritis by *in situ* hybridization. *Arthritis Rheum* 1995, 38:976-984
12. Koch AE, Burrows JC, Haines GK, Carlos TM, Harlan JM, Leibovich SJ: Immunolocalization of endothelial and leukocyte adhesion molecules in human rheumatoid and osteoarthritic synovial tissues. *Lab Invest* 1991, 64:313-320
13. Wilkinson LS, Edwards JCW, Poston RN, Hascard DO: Expression of vascular cell adhesion molecule-1 in normal and inflamed synovium. *Lab Invest* 1993, 68:682-688
14. Kriegsmann J, Keyszer GM, Geiler T, Bräuer R, Gay RE, Gay S: Expression of vascular cell adhesion molecule-1 mRNA and protein in rheumatoid arthritis synovium demonstrated by *in situ* hybridization and immunohistochemistry. *Lab Invest* 1995, 72:209-213
15. Fassbender HG: Histomorphologic basis of articular cartilage destruction in rheumatoid arthritis. *Coll Relat Res* 1983, 3:141-155
16. Müller-Ladner U, Kriegsmann J, Gay RE, Gay S: Oncogenes in rheumatoid arthritis. *Rheum Dis Clin N Am* 1995, 21:675-690
17. Brinckerhoff CE, Harris ED: Survival of rheumatoid synovium implanted into nude mice. *Am J Pathol* 1981, 103:411-419
18. Dodge GR, Jimenez S: An *in vitro* model of synovial cell adhesion and invasiveness into human articular cartilage. *Arthritis Rheum* 1994, 37:S311
19. Ramachandrala M, Tiku K, Tiku ML: Tripeptide RGD-

- dependent adhesion of articular chondrocytes to synovial fibroblasts. *J Cell Sci* 1992, 101:859–871
20. Geiler T, Kriegsmann J, Keyszer G, Gay RE, Gay S: A new model for rheumatoid arthritis generated by engraftment of rheumatoid synovial tissue and normal human cartilage into SCID mice. *Arthritis Rheum* 1994, 37:1664–1671
 21. Höyhty M, Myllylä R, Piuva J, Kivirikko KI, Tryggvason K: Monoclonal antibody to human prolyl 4-hydroxylase. *Eur J Biochem* 1984, 141:477–482
 22. Müller-Ladner U, Kriegsmann J, Tschopp J, Gay RE, Gay S: Demonstration of granzyme A and perforin mRNA in synovium of patients with rheumatoid arthritis. *Arthritis Rheum* 1995, 38:477–484
 23. Gay S, Fine JD: Characterization and isolation of polyclonal and monoclonal antibodies against collagen for use in immunohistochemistry. *Methods Enzymol* 1987, 145:148–167
 24. Firestein GS, Yeo M, Zvaifler NJ: Apoptosis in rheumatoid arthritis synovium. *J Clin Invest* 1995, 96:1631–1639
 25. Rendt KE, Barry TS, Jones DM, Richter CB, McCachren SS, Haynes BF: Engraftment of human synovium into severe combined immune deficient (SCID) mice: migration of human peripheral blood T-cells to engrafted human synovium and to mouse lymph nodes. *J Immunol* 1993, 151:7324–7336
 26. Aicher WK, Heer AH, Trabandt A, Bridges SL Jr, Schroeder HW Jr, Stransky G, Gay RE, Eibel H, Peter HH, Siebenlist U, Koopman WJ, Gay S: Overexpression of zinc-finger transcription factor Z-225/Egr-1 in synoviocytes from rheumatoid arthritis patients. *J Immunol* 1994, 152:5940–5948
 27. Lemaire R, Flipo R-M, Monte D, Dupressoir T, Duquesnoy B, Chesbron J-Y, Janin A, Capron A, Lafyatis R: Synovial fibroblast-like cell transfection with the SV40 large T antigen induces a transformed phenotype and permits transient tumor formation in immunodeficient mice. *J Rheumatol* 1994, 21:1409–1419
 28. Taniguchi S, Nishimura T, Takahashi T, Baba T, Kato K: Augmented excretion of preprocathepsin L of a fos-transferred highly metastatic cell line. *Biochem Biophys Res Commun* 1990, 168:520–526
 29. Elices MJ, Osborn L, Takada Y, Crouse C, Luhowskyi S, Hemler ME, Lobb RR: VCAM-1 on activated endothelium interacts with the leukocyte integrin VLA-4 at a site distinct from the VLA-4/fibronectin binding site. *Cell* 1990, 60:577–584
 30. Van Dinther-Janssen ACHM, Horst E, Koopman G, Newman W, Scheper RJ, Meijer CLJM, Pals ST: The VLA-4/VCAM-1 pathway is involved in lymphocyte adhesion to endothelium in rheumatoid synovium. *J Immunol* 1991, 147:4207–4210
 31. Elices M, Tsai V, Strahl D, Goel AS, Tollefson V, Arrhenius T, Wayner EA, Gaeta FCA, Fikes JD, Firestein GS: Expression and functional significance of alternatively spliced CS-1 fibronectin in rheumatoid arthritis microvasculature. *J Clin Invest* 1994, 93:405–416
 32. Müller-Ladner U: T cell independent pathways in rheumatoid arthritis. *Curr Opin Rheumatol* 1995, 7:222–228